Local magnetic moments in bcc Co

L. M. Sandratskii and J. Kübler
Institut für Festkörperphysik, Technische Hochschule, D-6100 Darmstadt, Germany
(Received 16 September 1992)

Recently developed density-functional methods are briefly reviewed and used to determine the band structure and total energy for noncollinear magnetic configurations in Co assuming different crystal structures. We thus examine configurations with continuously varying angles between the magnetic moments and obtain results for the stability of the magnetic moment in bcc, fcc, and hcp Co. We compare with Fe and Ni and find the moment to depend distinctly on the crystal structure, a fact that is shown to be related with typical, structure-dependent features of the densities of states.

I. INTRODUCTION

The possibility to grow successfully single-crystal films of bcc Co on different substrates[1,2] has opened interesting and new frontiers for experimental and theoretical studies. Thus several band-structure calculations were carried out for ferromagnetic bcc Co (e.g., Refs. 3–7) which showed that its band structure is similar to that of bcc Fe, the differences being mainly due to the shifted Fermi energy. This was supported experimentally by angle- and spin-resolved photoemission[8] which yields results that are in good agreement with the calculated band structure.

In a recent paper,[9] Singh focused attention on the experimentally determined fact[10,11] that Co atoms in bcc Fe-Co alloys possess magnetic moments which stay nearly unchanged regardless of the concentration of Co. Furthermore, the fact that the experimental value for the exchange stiffness constant of bcc-coordinated Co can be estimated successfully using the local-moment picture[12] lends weight to the latter's validity. Therefore, Singh[9] supposed that the magnetism of bcc Co should be described within the local-moment picture. To test the validity of this statement he carried out self-consistent calculation for antiferromagnetic bcc Co and obtained a substantial reduction of the moment in the antiferromagnetic state, leading him[9] to conclude that the local-moment picture is not likely to provide a good description of the magnetism in bcc Co, after all.

However, modern theories of itinerant electron magnetism[13,14] suppose that the angles between adjacent magnetic moments can assume arbitrary values, which implies that the probability of configurations with angles close to 180° is small. Thus comparing magnetic moments for only two magnetic configurations (ferromagnetic and antiferromagnetic) cannot give a valid picture of the stability of the atomic moments.

The recently developed methods that allow a determination of the band structure and total energy for noncollinear magnetic configurations[15–17] enable us to examine configurations with continuously varying angles between moments. A number of calculations was carried out to obtain the angular dependence of the atomic moments in Fe (Refs. 14, 18 and 19) and Ni.[20] In recent work[21] devoted to the calculation of the non-uniform magnetic susceptibility we reported data for fcc Co and hcp Co. In the present paper we discuss bcc Co. A comparison of results for different elements and crystal structures is carried out to understand the effects that influence the stability of the magnetic moments. We relate the angular dependence of the magnetic moments to properties of the electron density of states (DOS). It is shown that the similarity between band structures of bcc Co and bcc Fe also holds for noncollinear spin configurations.

II. CALCULATIONAL APPROACH

To make this paper reasonably self-contained we give a brief description of the main ideas underlying the theoretical method, stressing those points that distinguish it from conventional band-structure theory. At the basis is the local approximation to exchange and correlation[22] and the augmented spherical wave method (ASW) to carry out the self-consistent band-structure calculations.[23] This method was generalized by Uhl, Sandratskii, and Kübler[17] to enable the treatment of spiral spin configurations.

The effective single-particle Hamiltonian for spin-polarized electrons forming a noncollinear magnetic structure may be written as[17]

$$H = -\Delta + \sum_n U_n^{\dagger} V(|\mathbf{r} - \mathbf{R}_n|)\, U_n, \tag{1}$$

where

$$V(r) = \begin{pmatrix} V_+(r) & 0 \\ 0 & V_-(r) \end{pmatrix} \tag{2}$$

is a potential in the local atomic frame of reference which is defined by having the z axis parallel to the directions of the atomic moments. We shall call this the local coordinate system which may, in general, be different for each atom and which must be distinguished from the single, global coordinate system. The potentials V_σ ($\sigma = +, -$) are unambiguously given in the local coordinate system by means of functional derivatives[17,24] and the standard spin-$\frac{1}{2}$-rotation matrices U determine the transformation between the global coordinate system and the atomic systems.[17]

A spiral magnetic structure is defined by

$$\mathbf{m}_n = m\,(\cos(\mathbf{q}\cdot\mathbf{R}_n)\sin\vartheta, \sin(\mathbf{q}\cdot\mathbf{R}_n)\,\sin\vartheta, \cos\vartheta), \tag{3}$$

where $\mathbf{m}_n$ is the magnetic moment of the n-th atom and $(\mathbf{q}\cdot\mathbf{R}_n)$, ϑ are polar coordinates. It may easily be shown[25,26] that the Hamiltonian (1) commutes with the operator $\{\alpha_n(\mathbf{q}), \mathbf{R}_n\}$ of a generalized translation defined by

$$\{\alpha_n(\mathbf{q}), \mathbf{R}_n\}\,\psi(\mathbf{r}) = \begin{pmatrix} \exp\left(-\frac{1}{2}\,i\,\mathbf{q}\cdot\mathbf{R}_n\right) & 0 \\ 0 & \exp\left(\frac{1}{2}\,i\,\mathbf{q}\cdot\mathbf{R}_n\right) \end{pmatrix} \psi(\mathbf{r}-\mathbf{R}_n)\ . \tag{4}$$

The quantity $\psi(\mathbf{r})$ is a bispinor function and the operators $\{\alpha_n(\mathbf{q}), \mathbf{R}_n\}$ combine a space translation through the vector $\mathbf{R}_n$ with a spin rotation about the global axis by the angle $(\mathbf{q}\cdot\mathbf{R}_n)$. These generalized translations form an Abelian group isomorphic to the group of ordinary space translations by vectors $\mathbf{R}_n$. Therefore, the irreducible representations of both groups coincide, and for the eigenfunctions of the Hamiltonian (1), there exists a generalized Bloch theorem

$$\{\alpha_n(\mathbf{q}), \mathbf{R}_n\}\,\psi_{\mathbf{k}}(\mathbf{r}) = \exp(-i\,\mathbf{k}\cdot\mathbf{R}_n)\,\psi_{\mathbf{k}}(\mathbf{r}), \tag{5}$$

where the vectors $\mathbf{k}$ lie in the first Brillouin zone, which is defined in the usual way by the vectors $\mathbf{R}_n$. This means that for the actual calculations one only needs the chemical unit cell in contrast to a supercell.

The usual ansatz for a band-structure calculation is the expansion of the Bloch bispinor function in the form

$$\psi_{\mathbf{k}}(\mathbf{r}) = \sum_{L\sigma} C_{L\sigma}\,\Phi_{L\sigma\mathbf{k}}(\mathbf{r}), \tag{6}$$

where, because of Eq. (5), $\Phi_{L\sigma\mathbf{k}}$ may be written as a lattice sum

$$\Phi_{L\sigma\mathbf{k}}(\mathbf{r}) = \sum_n \exp(i\,\mathbf{k}\cdot\mathbf{R}_n)\,U_n^{\dagger}\,\phi_{L\sigma}(\mathbf{r}-\mathbf{R}_n). \tag{7}$$

L denotes both angular momentum quantum numbers l and m, and $\sigma = 1, 2$, two possible bispinors $\phi_{L\sigma}$. Within the ASW method the latter are constructed using augmented spherical waves essentially as described before.[17,24] Of course, other methods such as the linear muffin-tin orbital (LMTO)[16,27] may be used instead. A standard Rayleigh-Ritz variational procedure now leads to the secular equation for spiral magnetic structures.[17]

At this point it is worthwhile to stress a basic difference between the band structure of a ferromagnet and of a crystal with noncollinear magnetic order.[18,17] In a ferromagnet each electron state is specified by a definite spin projection on the magnetization axis and calculations for electron states with opposite spin projections can be carried out separately. For noncollinear magnetic configurations the spin projection is no longer a good quantum number, and the electron wave functions contain contributions from both spin projections. This leads to a doubling of the dimension of the secular matrix and allows a description of the variation of the electron states at the transition from the ferromagnetic to noncollinear structures in terms of hybridization of states with opposite spin projections.

To investigate the stability of magnetic moments we are to take into account excited states of the system. These can be obtained in basically two different ways. First, different values of the angles between adjacent magnetic moments are specified by different values of the wave vector $\mathbf{q}$ and for different values of $\mathbf{q}$ the magnetic moment, in general, is different. Thus, besides possibly the ground state, we obtain excited states by carrying out self-consistent calculations as a function of the wave vector $\mathbf{q}$. Second, the magnitude of the moment may be varied keeping the value of $\mathbf{q}$ fixed. But since a routine self-consistent calculation gives the state with lowest energy, the calculations must now be carried out for the system in an external magnetic field which stabilizes the state with higher energy. Applying to a magnetic state of the form (3) an external field having the same configuration, we will obtain a new state of the form (3) but with higher energy. The details of the corresponding calculational technique may be found in Ref. 21. The total energy of excited states characterized by the local magnetic moment m may be represented in the approximated form[21]

$$E_{\mathbf{q}}(m) = E_{\mathbf{q}}\,(m_0(\mathbf{q})) + \frac{1}{2\chi(\mathbf{q})}\,[m - m_0(\mathbf{q})]^2\ , \tag{8}$$

where $m_0(\mathbf{q})$ is the self-consistent magnetic moment in the absence of the magnetic field, $E_{\mathbf{q}}(m_0(\mathbf{q}))$ is the total energy of this state calculated with usual procedure[24] of local density functional theory, and $\chi_{\mathbf{q}}$ is the magnetic susceptibility. The smaller the susceptibility, the steeper is the energy minimum for this $\mathbf{q}$ and, correspondingly, the weaker are fluctuations of the magnetic moment.

All calculations described in the next section were carried out for spiral structures (3) with an angle ϑ equal to 90° and the wave vector $\mathbf{q}$ was varied along the (001) axis. Parameters of the calculations and some selected results are collected in Table I.

III. RESULTS AND DISCUSSION

We start with a discussion of the behavior of $m_0(\mathbf{q})$. The calculational results for different crystal structures of Co as well as a comparison with results for bcc Fe and fcc Ni are given in Figs. 1–3 . In all cases we see a tendency of the magnetic moment to decrease with increasing q, i.e., increasing angles between the magnetic moments of adjacent atoms. The rate of change is small

TABLE I. Parameters and selected results of calculations for bcc, fcc, and hcp Co. Here $m_0(0)$ is the atomic spin moment in the ferromagnetic configuration, $\chi(0)$ is the spin susceptibility in the ferromagnetic configuration, and D is the exchange stiffness. For comparison the parameters of Singh (Ref. 9) and some experimental data are also given.

	Lattice	Lattice parameters	$m_0(0)$ (μ_B)	χ (0) (μ_B/Ry)	$\frac{D_{hcp}}{D_{bcc}}$
This study	bcc	2.82	1.72	8.0	
Singh[a]	bcc	2.76	1.73	8.4	
Experiment	bcc	2.82[b]	1.3–1.7[c]		
This study	fcc	3.41	1.54	10.6	
This study	hcp	2.51 4.07	1.54	7.2	
This study					1.53
Experiment					1.55[d]

[a] Reference 9.
[b] Reference 2.
[c] References 12, 28, and 29.
[d] Reference 12.

for small q but rises for larger q. In particular, the magnetic moment of bcc Co at q=0.3, corresponding to an average angle between adjacent atomic moments equal to 54°, remains at 90% of the ferromagnetic value. In a comparison of the data for different crystal structures of Co one should take into account that for the same value of q the average angles between adjacent atomic moments for bcc, hcp, and fcc structures have the relation 2:1.5:1 . We conclude that the slowest decrease of the magnetic moment with increasing angle is observed in the case of the bcc structure and the fastest decrease in the case of the fcc structure. For fcc Co the self-consistent value of the magnetic moment is zero from $q = 0.6$ onwards, corresponding to an angle of 72° (and larger) between moments.

We extend the comparison over different elements and give in Figs. 1 and 2 the $m_0(q)$ data for bcc Fe and fcc Ni, respectively. These results confirm our conclusion that the crystal structure with the most stable magnetic moment is bcc. In view of the large difference between the ferromagnetic moments of fcc Co and fcc Ni, it is quite remarkable that the scaled $m_0(q)$ curves are so similarly

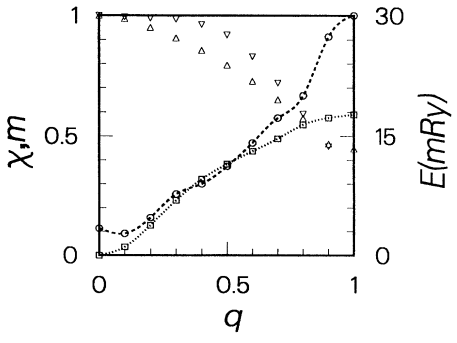

FIG. 1. **q** dependence of the local magnetic moment (△), total energy (□), and susceptibility (○) of bcc Co. For comparison the **q** dependence of the local magnetic moment of bcc Fe (▽) is also represented. Magnetic moments are given in units of $m_0(0)$, susceptibility in units of $\chi_{max} = 70.5\mu_B$/Ry. The length of the **q** vector is given in units of $2\pi/a$.

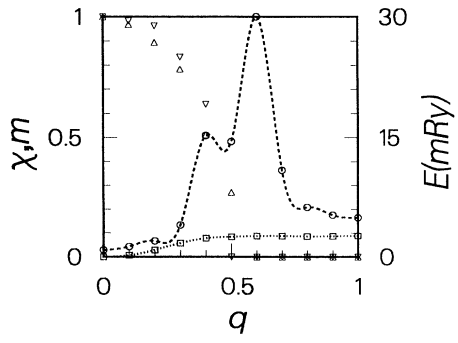

FIG. 2. **q** dependence of the local magnetic moment (△), total energy (□), and susceptibility (○) of fcc Co. For comparison the **q** dependence of the local magnetic moment of fcc Ni (▽) is also represented. Magnetic moments are given in units of $m_0(0)$, susceptibility in units of $\chi_{max} = 371.5\mu_B$/Ry. The length of the **q** vector is given in units of $2\pi/a$.

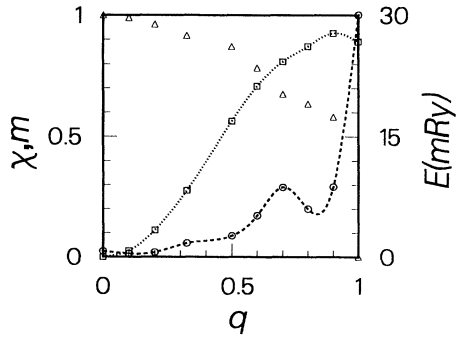

FIG. 3. **q** dependence of the local magnetic moment (△), total energy (□), and susceptibility (○) of hcp Co. Magnetic moments are given in units of $m_0(0)$, susceptibility in units of $\chi_{max} = 309.7\mu_B/\text{Ry}$. The length of the **q** vector is given in units of $2\pi/a$.

characterized by the fast decrease of the magnetic moments.

To provide an explanation of the observed relation between the angular behavior of the magnetic moment and the crystal structure we now analyze the angular dependence of the density of states and show in Fig. 4 the DOS for bcc Co. The ferromagnetic DOS [Fig. 4(a)] may be subdivided into three energy regions: Below 0.53 Ry (range I) there occur preferential states with a positive spin projection, between 0.53 and 0.69 Ry (range II) there are states of both spin projections, and above 0.69 Ry (range III) there occur preferential states with a negative spin projection. In all regions the state densities form clear-cut peaks with deep minima between them.

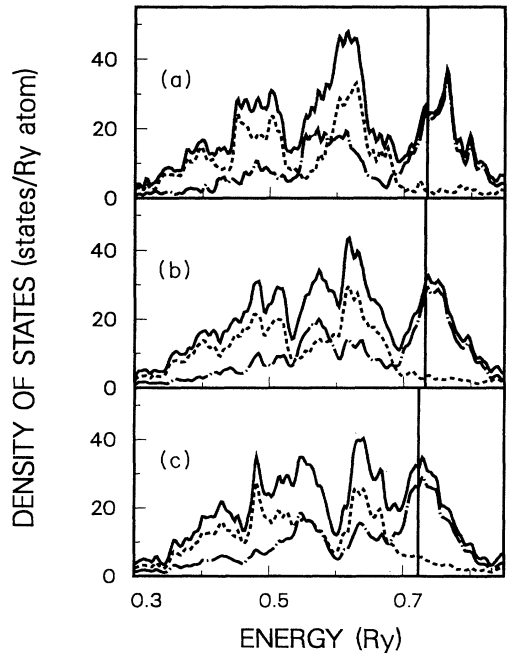

FIG. 4. Density of states of bcc Co for configurations with different angles between nearest atomic moments: (a) 0, (b) 36°, and (c) 72°. The solid line shows the total DOS, the dashed and dot-dashed lines, correspondingly, spin-up and spin-down decomposed densities of states. The Fermi energy is marked by a vertical line.

When the atomic moments deviate from parallel alignment, the spin projection is no longer a good quantum number (see Sec. II). Still, in the energy ranges I and III the electron states continue to have mostly contributions of the spin projection that is parallel to the local magnetic moments for range I and antiparallel for range III. Cardinal changes occur in region II where hybridization and "hybridization repulsion" of states, characterized by a high-d contribution and opposite spin indices, cause the total-DOS peak [Fig. 4(a)] to split into individual peaks [Figs. 4(b) and (c)]. Therefore the most outstanding feature that distinguishes the three DOS curves is the splitting of the prominent peak at 0.61 Ry in Fig. 4(a) into two peaks that become more distinct with increasing angles [Figs. 4(b) and (c)].

As the Fermi energy belongs to the region III of the DOS the remarkable changes in the region II do not influence the value of the atomic moments because they do not change the number of occupied spin-up and spin-down states. The decrease of the moment is connected with an essentially weaker effect of the increasing admixture of the spin-up states to the spin-down states of the region III, which is also a result of the interaction of opposite spin states in a noncollinear structure. However, because of the large energy distance and deep minimum between the spin-down peak in range III and spin-up peak in range II the admixture increases rather slowly, leading to relative stability of the atomic magnetic moment.

The angular variation of the DOS of bcc Co is very similar to the variation of the DOS of bcc Fe obtained earlier in Ref. 18 and applied to the explanation of the experimental temperature dependence of the x-ray photoemission spectrum in a recent paper.[30] The higher stability of the local magnetic moment of bcc Fe in a wide angular interval from 0 to 90° (Fig. 1) is connected with the difference in the position of the Fermi level. Indeed, in bcc Fe the Fermi level lies in the valley between energy regions II and III and the hybridizational changes discussed above do not disturb the balance of the occupied spin-up and spin-down states.

To understand the difference in angular dependence of the magnetic moments for different crystal lattices we consider in Fig. 5 the DOS of fcc Co for a number of magnetic configurations. Both bcc and fcc modifications of Co in the ferromagnetic phase have rather close values of the atomic magnetic moment and, correspondingly, rather close values of the exchange splitting, which may be estimated as an energy difference between the corresponding spin-up and spin-down peaks of the DOS. However, in contrast to the case of bcc Co, the DOS of fcc Co cannot be subdivided into clear-cut separate peaks with deep minima between them. As all spin-up d states are occupied, the position of the Fermi level, for both lattices, is determined by the upper part of spin-down d states. In bcc Co these states form a separated peak at a substantial energy distance away from the upper part of

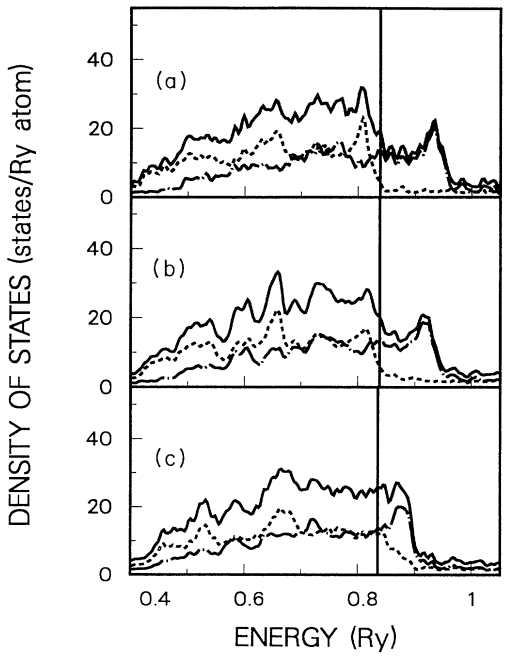

FIG. 5. Density of states of fcc Co for configurations with different angles between nearest atomic moments: (a) 0, (b) 36°, and (c) 72°. The solid line shows the total DOS, the dashed and dot-dashed lines, correspondingly, spin-up and spin-down decomposed densities of states. The Fermi energy is marked by a vertical line.

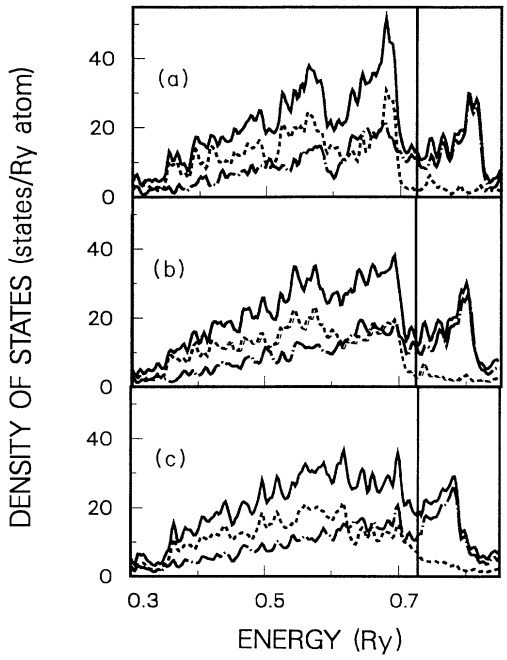

FIG. 6. Density of states of hcp Co for configurations with different angles between nearest atomic moments: (a) 0, (b) 36°, and (c) 72°. The solid line shows the total DOS, the dashed and dot-dashed lines, correspondingly, spin-up and spin-down decomposed densities of states. The Fermi energy is marked by a vertical line.

spin-up states. As a result, the noncollinearity of magnetic moments does not lead to a fast increase of the spin-up admixture to the empty spin-down states and, therefore, to a fast decrease of magnetic moment.

In the case of fcc structure d states are distributed more uniformly, resulting in essentially less distance between the Fermi level and upper part of the occupied spin-up states. Because of this small distance the noncollinearity of magnetic moments leads to intensive mixing between occupied spin-up states and empty spin-down states. An increased contribution of spin-up states to the unoccupied part of the DOS determines the decreasing of the magnetic moment. This effect is clearly seen in Fig. 5. Indeed, in the ferromagnetic case [Fig. 5(a)] there is a sharp peak of the spin-up DOS about 0.3 Ry below the Fermi energy and very low spin-up DOS above E_F. With increasing angles between atomic moments [Figs. 5(b)–5(d)] we observe a "smearing" of the peak and, correspondingly a substantial increase of the spin-up DOS above E_F.

The DOS of hcp Co (Fig. 6) has some properties of both bcc and fcc Co, resulting in an intermediate level of the stability of the magnetic moment in this case. The peaks of the ferromagnetic DOS [Fig. 6(a)] are better defined than in the case of the fcc lattice: The peaks are higher, with deeper minima between them. However, as compared with bcc Co there are more peaks and the energy distance between them is less. In particular, the Fermi level is much closer to spin-up states than in the bcc structure. With increasing angles the peaks of the DOS of the hcp structure lose their individuality and form a more uniform d band. The spin-up admixture to empty spin-down states is analogous to that discussed for fcc Co and leads to decreasing magnetic moments. However, this process is slower here than for the fcc structure. Note that the features of the DOS referred to here are quite well known[31] and are characteristics of the different crystal structures.

To complete the picture we comment on results for the total energy, calculated with Eq. (8). We begin by noting that by means of the $E_{\mathbf{q}}$ $(m_0(\mathbf{q}))$ function the exchange stiffness constant D may be estimated.[32] In Table I we compare the theoretical and experimental[12] ratios of the exchange stiffness constants of hcp Co and bcc Co. Theory and experiment are in very good agreement. The closeness of $\frac{D_{\rm hcp}}{D_{\rm bcc}}$ to the ratio $\frac{3}{2}$ of the numbers of nearest neighbors in the hcp and bcc structures leads Singh[9] to the conclusion that magnetism of Co may probably be described in terms of the nearest-neighbor Heisenberg model of local moments. However, the closeness of $\frac{D_{\rm hcp}}{D_{\rm bcc}}$ to $\frac{3}{2}$ seems to us accidental because for $\mathbf{q}$ parallel to the z axis, used in our calculations, all atoms belonging to the same xy plane have parallel magnetic moments and thus do not contribute to increase the total energy, within the nearest-neighbor Heisenberg model. Because of this property, in the case of hcp structure only 6 of 12 nearest neighbors give a contribution to the increase of the total energy in contrast to the bcc structure where all 8 nearest neighbors of an atom contribute to change the total

energy. Therefore in the case considered the ratio of the "effective" numbers of nearest neighbors in hcp and bcc lattices is 6:8 but not 12:8, which is necessary to give the simple interpretation of the value of $\frac{D_{\rm hcp}}{D_{\rm bcc}}$.

For all crystal structures (Figs. 1–3) investigated here the total energy $E_{\mathbf{q}}$ $(m_0(\mathbf{q}))$ shows the tendency to increase with increasing q. However, for fcc Co (Fig. 2) this increase is weaker and ends at q equal to 0.6 where the magnetic moment $m_0(\mathbf{q})$ vanishes. We obtained the $E_{\mathbf{q}}$ $(m_0(\mathbf{q}))$ function for Ni before[21] and now state that it is remarkably similar to the $E_{\mathbf{q}}$ $(m_0(\mathbf{q}))$ function for Co in spite of the large difference of their ferromagnetic moments, viz. $0.56\mu_B$ and $1.54\mu_B$. Because of this we may safely suppose that fluctuations of the directions of the local magnetic moments in fcc Co are much stronger than in bcc and hcp Co.

Information on amplitude fluctuations of atomic moments may be obtained from the longitudinal susceptibility. For all lattices considered (Figs. 1–3) the susceptibility for the ferromagnetic configuration is small. This means that for configurations with small angles longitudinal fluctuations are weak. For example, using (8) we can estimate the variation of the magnetic moment of bcc Co corresponding to an energy change of the order of 1000 K as not exceeding $0.1\mu_B$. However, with increasing q there is a tendency for the longitudinal susceptibility to increase. The susceptibility is especially large near the points where the self-consistent moment $m_0(q)$ vanishes ($q = 0.6$ for fcc Co and $q = 1.0$ for hcp Co). This means that for these magnetic configurations the total energy (8) depends weakly on the lengths of the magnetic moments and fluctuations of them are very strong.

IV. CONCLUSION

Taking up a line started by Singh,[9] we extended the examination of the stability of the atomic magnetic moments in bcc Co by considering noncollinear magnetic configurations; this allowed us to investigate the value of the magnetic moment as a function of continuously varying angles between atomic moments. We summarize the results of our calculations by stating that the character of the angular variation of the local magnetic moments depends distincly on the crystal structure. In the cases considered the moment is most stable for the bcc structure and least stable for the fcc structure. We related this behavior with typical, structure-dependent properties of the ferromagnetic density of states.

Our extension of Singh's[9] treatment is also of importance for the study of the principal role of fluctuations of the local magnetization in determining thermodynamic properties of itinerant magnets. However, to describe the stability of magnetic moments quantitatively a consistent statistical mechanics theory must be used which allows, on the basis of results of *ab initio* band-structure calculations, a reliable estimate of the temperature dependence of short-range magnetic order and therefore of the average angles between atomic moments. Although progress in the statistical mechanics theory of itinerant electron magnets was achieved within the last years, this topic is still controversial and different theories give essentially different estimates of the main physical parameters, in particular, of the short-range magnetic order. In the present paper we did not touch this very difficult problem, but restricted ourselves to a qualitative discussion.

ACKNOWLEDGMENTS

One of us (L.M.S.) gratefully acknowledges financial support by the Alexander von Humboldt-Stiftung (Bonn). We have received support by the DFG under the auspices of SFB 252, Darmstadt/Frankfurt/Mainz.

[1]G.A. Prinz, Phys. Rev. Lett. **54**, 1051 (1985).
[2]Y.U. Idzerda, W.T. Elam, B.T. Jonker, and G.A. Prinz, Phys. Rev. Lett. **62**, 2480 (1989).
[3]D. Bagayoko, A. Ziegler, and J. Callaway, Phys. Rev. B **27**, 7046 (1983).
[4]K. Schwarz, P. Mohn, P. Blaha, and J. Kübler, J. Phys. F **14**, 2659 (1984).
[5]F. Hermann, P. Lambin, and O. Jepsen, Phys. Rev. B **31**, 4394 (1985).
[6]V.L. Moruzzi, P.M. Marcus, K. Schwarz, and P. Mohn, Phys. Rev. B **34**, 1784 (1986).
[7]J.I. Lee, C.L. Fu, and A.J. Freeman, J. Magn. Magn. Mater. **62**, 93 (1986).
[8]G.A. Prinz, E. Kisker, K.B. Hathaway, K. Schroder, and K.H. Walker, J. Appl. Phys. **57**, 3024 (1985).
[9]D.J. Singh, Phys. Rev. B **45**, 2258 (1992).
[10]M.F. Collins and J.B. Forsyth, Philos. Mag. **8**, 401 (1963).
[11]S. Spooner, J.W. Lynn, and J.W. Cable, in *Magnetism and Magnetic Materials 1971 (Chicago)*, Proceedings of the 17th Annual Conference on Magnetism and Magnetic Materials, edited by D.C. Graham and J.J. Ryne, AIP Conf. Proc. No. 5 (AIP, New York, 1972), p. 1415.
[12]J.M. Karanikas, R. Sooryakumar, G.A. Prinz, and B.T. Jonker, J. Appl. Phys. **69**, 6120 (1991).
[13]T. Moriya, *Spin Fluctuations in Itinerant Electron Magnetism* (Springer, Berlin,1985); *Metallic Magnetism*, edited by H. Capellmann (Springer, Berlin, 1987); V. Korenman, J.L. Murray, and R.E. Prange, Phys. Rev. B **16**, 4032 (1977); J. Hubbard, *ibid.* **20**, 4584 (1979); B.L. Gyorffy, A.J. Pindor, J. Staunton, G.M. Stocks, and H. Winter, J. Phys. F **15**, 1337 (1985).
[14]M.V. You and V. Heine, J. Phys. F **12**, 177 (1982).
[15]L.M. Sandratskii, Phys. Status Solidi B **135**, 167 (1986).
[16]O.N. Mryasov, A.I. Liechtenstein, L.M. Sandratskii and V.A. Gubanov, J. Phys. Condens. Matter **3**, 7683 (1991).
[17]M. Uhl, L.M. Sandratskii and J. Kübler, J. Magn. Magn. Mater. **103**, 314 (1992).
[18]L.M. Sandratskii and P.G. Guletskii, J. Magn. Magn. Mater. **79**, 306 (1989).
[19]M.U. Luchini, and V. Heine, J. Phys. Cond. Matter **1**, 8961 (1989).
[20]E.M. Haines, Solid State Commun. **69**, 561 (1989).

[21]L.M. Sandratskii and J. Kübler, J. Phys. Condens. Matter **4**, 6927 (1992).
[22]W. Kohn and L.J. Sham, Phys. Rev. **140**, A1133 (1965); U. von Barth and L. Hedin, J. Phys. C **5**, 1629 (1972).
[23]A.R. Williams, J. Kübler, and C.D. Gelatt, Phys. Rev. B **19**, 6094 (1979).
[24]J. Sticht, K.H. Höck, and J. Kübler, J. Phys. Condens. Matter **1**, 8155 (1989).
[25]C. Herring, in *Magnetism*, edited by G. Rado and H. Suhl (Academic, New York, 1966).
[26]L.M. Sandratskii, J. Phys. Condens. Matter **3**, 8565 (1991); **3**, 8587 (1991).
[27]O.K. Andersen, Phys. Rev. B **12**, 3060 (1975).
[28]J.A.C. Bland, R.D. Baterson, P.C. Riedi, R.G. Graham, H.J. Lauter, J. Penford, and C. Shackleton, J. Appl. Phys. **69**, 4989 (1981).
[29]P.C. Riedi, T. Dumelow, M. Rubenstein, G.A. Prinz, and S.B. Qadri, Phys. Rev. B **36**, 4595 (1987).
[30]L.M. Sandratskii, J. Kübler, and E. Kisker, Solid State Commun. **83**, 559 (1992).
[31]J. Kübler and V. Eyert, in *Electronic and Magnetic Properties of Metals and Ceramics*, edited by K.H.J. Buschow (VCH-Verlag, Weinheim, 1992), p. 1.
[32]A.J. Holden and M.V. You, J. Phys. F **12**, 195 (1982).